

RESEARCH ARTICLE

Lornoxicam controlled release transdermal gel patch: Design, characterization and optimization using co-solvents as penetration enhancers

Durriya Hashmat, Muhammad Harris Shoaib^{*}, Fatima Ramzan Ali, Fahad Siddiqui

Department of Pharmaceutics, Faculty of Pharmacy and Pharmaceutical Sciences, University of Karachi, Karachi, Pakistan

* harrishshaib2000@yahoo.com, mhshoaib@uok.edu.pk



Abstract

The aim of the current study was to develop membrane-based transdermal patches of lornoxicam gel using oleic acid (OA) and propylene glycol (PG) as penetration enhancers to improve drug delivery across the skin and to evaluate in vivo analgesic and anti-inflammatory activity. For this purpose, nine formulations were developed in accordance with 3^2 factorial design using Design Expert[®] 11. The concentration of propylene glycol (X_1) and oleic acid (X_2) were selected as independent variables whereas Q_{10} (Y_1), flux (Y_2) and lag time (Y_3) were considered as the response variables. The impact of drug loading, surface area, gel concentration, membrane variation and agitation speed on drug release and permeation was also studied. The skin sensitivity reaction, analgesic activity and anti-inflammatory action of the optimized patch were also determined in Albino Wistar rats. Stability studies were performed for three months at three different temperature conditions. The result suggests that a membrane-based system with controlled zero-order drug release of $95.8 \pm 1.121\%$ for 10 h exhibiting flux of $126.51 \pm 1.19 \mu\text{g}/\text{cm}^2/\text{h}$ and lag time of $0.908 \pm 0.57\text{h}$ was optimized with the desired analgesic and anti-inflammatory effect can be obtained by using propylene glycol and oleic acid co-solvents as a penetration enhancer. The patch was also found stable at 4°C for a period of 6.44 months. Formulation F9 comprising of 10% PG and 3% OA was selected as an optimized formulation. The study demonstrates that the fabricated transdermal system of lornoxicam can deliver the drug through the skin in a controlled manner with desired analgesic and anti-inflammatory activity and can be considered as a suitable alternative of the oral route.

OPEN ACCESS

Citation: Hashmat D, Shoaib MH, Ali FR, Siddiqui F (2020) Lornoxicam controlled release transdermal gel patch: Design, characterization and optimization using co-solvents as penetration enhancers. PLoS ONE 15(2): e0228908. <https://doi.org/10.1371/journal.pone.0228908>

Editor: Rona Chandrawati, University of New South Wales, AUSTRALIA

Received: March 18, 2019

Accepted: January 6, 2020

Published: February 27, 2020

Copyright: © 2020 Hashmat et al. This is an open access article distributed under the terms of the [Creative Commons Attribution License](https://creativecommons.org/licenses/by/4.0/), which permits unrestricted use, distribution, and reproduction in any medium, provided the original author and source are credited.

Data Availability Statement: All relevant data are within the manuscript and its Supporting Information files.

Funding: The author(s) received no specific funding for this work.

Competing interests: The authors have declared that no competing interests exist.

Introduction

The nonsteroidal Anti-inflammatory Drugs (NSAIDs) have been extensively recommended for the treatment of inflammatory disorders including osteoarthritis and Rheumatoid arthritis. Oral administration of NSAIDs exhibits efficient relief in inflammatory diseases. However, the

adverse effects such as irritation and ulceration of gastro-intestinal mucosa have limited the clinical use of NSAIDs [1]. One of the approaches to avoid toxicity and using NSAIDs for a longer period of time is its administration via transdermal route.[2]

Transdermal systems by delivering drugs across the skin into systemic circulation resist the alteration in absorption rate, metabolism and prevent the gastrointestinal adverse effects occurring due to oral administration of drugs.[3, 4] It is ideally suited for chronic disorders. [5] It allows the administration of potent drugs with the benefit of self-administration and enhanced therapeutic efficacy.[6]

Lornoxicam (LRX) is a potent NSAID of oxicam class. It is extensively prescribed in chronic painful and inflammatory conditions. Like other NSAIDs, oral administration of LRX leads to numerous gastrointestinal, renal and hematological adverse effects.[7]. Apart from these, it needs frequent administration due to its short half-life (3-4h). Moreover, parenteral administration is not recommended against chronic conditions[8]

The controlled delivery of LRX through the transdermal route is an advantageous approach to overcome all the concerns associated with LRX administration. In the present study, LRX has been formulated as reservoir transdermal patches. The reservoir transdermal patches contain the drug in a separate compartment which can be delivered by a simple diffusion process providing controlled drug delivery over a required period of time. Since it follows zero order kinetics, there is an effective control on release rate.

The skin acts as an excellent barrier to the transdermal permeation of drugs. Different chemical enhancers have been introduced in order to enhance transdermal drug delivery. These chemical enhancers by interacting with the skin constituents improve the flux of drug molecules [9]. These agents reversibly alter the skin's barrier function and subsequently allow the molecules with poor penetration to surpass stratum corneum and ultimately enter the systemic circulation.[10] Numerous studies have shown that penetration enhancers, when used in combination can produce synergistic action thereby promoting skin permeation greater than individual penetration enhancers. [11]. Co-solvents have been extensively used as vehicles and penetration enhancers in transdermal formulations. These agents not only enhance the drug solubility but also alter the structure of the skin and hence improve the penetration rate. Thus, affecting both drug release and permeation.[12]

Many fatty acids have been used to improve percutaneous drug absorption including oleic acid (OA). The use of OA with propylene glycol (PG) proves to be a very successful combination in many transdermal formulations.[9, 13, 14]

Hence, the aim of the current study is to improve the transdermal permeation of LRX by using PG and OA co-solvent as a penetration enhancer. For this purpose, reservoir type transdermal patches of LRX has been developed using a rate-controlling membrane, which can control the release at a constant rate for a period of 10 h.

2. Materials and methods

2.1. Materials

Lornoxicam was gifted by ATCO Laboratories Ltd., Pakistan. Other chemicals/excipient used were Carbopol 940, oleic acid (OA) and Propylene Glycol (PG) (Dae-Jung, Gyeonggi-do, Korea), Triethanolamine (BDH, Poole, England) and Methanol HPLC grade (TEDIA, Fairfield, USA). The backing membrane (3M-9720), rate-controlling membranes (3M Cotran-9728 and 3M CoTran-9716) and release liner (SCOTCHPAK—9755) were gifted by 3M, St. Paul, USA. Acrylate adhesive Duro-Tak 387/2510 was supplied by Henkel Corporation (Bridgewater, USA).

2.2. Animals

The animals used for skin irritation and analgesic/anti-inflammatory studies were Male Wistar Albino Rats (weighing 150–180 g) provided by the animal house, Faculty of Pharmacy and Pharmaceutical Sciences, University of Karachi, Pakistan. All ARRIVE guidelines for the maintenance and utilization of laboratory animals were followed. The animals were kept under standard laboratory conditions with free access to food and water. All the protocols followed for animal studies were reviewed and approved by the Institutional Bioethics Committee, University of Karachi (IBC KU 51).

2.3. Solubility studies of lornoxicam

Excess quantity of LRX powder was taken in separate conical flasks containing 10 mL phosphate buffer saline (PBS) pH 5.8, pH 6.8, pH 7.4 and water. The flasks were continuously stirred for 72h using orbital shaker bath (Model SW-23, Julabo, USA). An aliquot was withdrawn and filtered using Millipore filter 0.45 μm . The dilution was analyzed spectrophotometrically at 376 nm. The concentration was determined in triplicate[15].

2.4. Experimental design

A 3^2 full factorial design was used to design the experiments using Design-Expert version 11 (Stat-ease Inc, Minneapolis, USA). PG (X_1) and OA (X_2) were selected as independent variables whereas drug release at 10h, Q_{10} (Y_1), flux (Y_2) and lag time (Y_3) were considered as dependent response variables. Nine formulations of gel were constructed as specified in Table 1. For each response, the polynomial equation was generated and from the results obtained, the optimized formulation was selected.

2.5. Formulation of lornoxicam gel

For the preparation of gel, carbopol was soaked in water overnight. Then, a measured quantity of LRX was dissolved in triethanolamine. Methylparaben, PG, OA and 10 mL of water were dissolved in the drug mixture with constant stirring. The solvent blend was mixed with carbopol and agitated for additional 20 minutes until a homogeneous gel was formed.[16]

2.6. Physicochemical characterization of lornoxicam gel

The prepared LRX gels were assessed for color, homogeneity, viscosity, pH and drug content. The pH was measured using a calibrated pH meter (Mettler MP-220, Switzerland). Brookfield viscometer (Model DV II, USA) was used to determine the viscosity of gel at 25°C; the spindle was set at 20 rpm. Each test was repeated in triplicate.

Table 1. Composition of lornoxicam gel for membrane-based transdermal patches.

Ingredients (% w/w)	Formulation Code								
	F1	F2	F3	F4	F5	F6	F7	F8	F9
Lornoxicam	0.8	0.8	0.8	0.8	0.8	0.8	0.8	0.8	0.8
Propylene glycol (PG)	15	5	15	5	10	5	10	15	10
Oleic acid (OA)	1	5	5	1	5	3	1	3	3
Methyl paraben	0.2	0.2	0.2	0.2	0.2	0.2	0.2	0.2	0.2
Triethanolamine	2	2	2	2	2	2	2	2	2
Carbopol (940)	0.5	0.5	0.5	0.5	0.5	0.5	0.5	0.5	0.5
Distilled water	100	100	100	100	100	100	100	100	100

<https://doi.org/10.1371/journal.pone.0228908.t001>

2.7. Dose calculation for transdermal formulation

The dose calculation for controlled drug delivery has been illustrated by Baker [17] which is given as:

$$t_e = t_{1/2} \frac{M_0 - M_e}{\ln 2 M_e} \quad (1)$$

Where, M_0 is a required dose of the drug, t_e is the required duration of action, M_e is Minimum effective concentration and $t_{1/2}$ is the half-life of the drug.

LRX has a minimum effective concentration of 1 mg/L with a half-life of 4h and volume of distribution of 14 L.[18]. The calculated dose used in the formulated patches was 38.22mg.

2.8. Fabrication of membrane-based lornoxicam patches

The reservoir-type TDS of LRX was fabricated by sandwiching the reservoir gel between the backing layer (3M -9720) and an ethylene-vinyl acetate (EVA) membrane (3M Cotran– 9728). First, the EVA membrane and the backing layer was heat sealed and cut to an appropriate size (30 cm²). Then, accurately weighed quantity of gel (5 g) was filled in the device by means of a disposable syringe. The device was heat-sealed again ensuring no leakage of the reservoir gel from the device. A pressure sensitive adhesive polymer (Duro-tak 387/2510) was coated onto the EVA membrane to ensure intimate contact of the patch to the skin. Finally, a release liner (Scotchpak—9755) was pressed over the adhesive coated rate-controlling membrane. The patches were stored in aluminum foil at room temperature.[19]

2.9. Characterization of fabricated patches

2.9.1. Weight. Three patches from each formulation were randomly selected and weighed individually. Then, the average weight and standard deviation were calculated. [20]

2.9.2. Thickness. The thickness of the patches was measured by means of a micrometer screw gauge at the 4 edges and the center of the patch. The results were expressed as average thickness \pm SD. [21]

2.9.3. Content uniformity of patches. *2.9.3.1. Sample preparation.* The reservoir compartment containing drug was extracted with 100 mL of PBS pH 7.4. The flask was stirred for 4 h using a mechanical shaker (IKA, KS 260 basic, Germany). The solution was filtered, and drug content was determined by the HPLC method.

2.9.3.2. HPLC analysis. The quantification of LRX was performed using the HPLC method described by Gonullu et al with minor modifications[7]. The HPLC unit was equipped with pump (Shimadzu 20AD), UV detector (Shimadzu SPD-20A, photo diode array (PDA) and C-18 column (250 \times 4.6 mm, 5 μ m particle size, Mediterranean Sea[®], Teknokroma, Barcelona, Spain). The samples were detected at 376 nm and data acquisition was performed using software (Lab solutions, Version 6.72 SP 1). The mobile phase consisted of aqueous phosphate buffer and methanol in a ratio of 6:4 v/v having a pH of 7 adjusted by 1 M sodium hydroxide. Its flow rate was 1 mL/min and the volume of sample injected was 20 μ L. The LOD and LOQ values were 0.1 and 0.5 μ g/mL, respectively.

A standard calibration curve of LRX was constructed in the range of 0.5–20 μ g/mL. To evaluate the linearity, drug determination was carried out in the mobile phase. Good linearity was observed between the concentration of lornoxicam and the peak area of lornoxicam with a high correlation coefficient ($r^2 = 0.999$). The standard curve constructed was used for estimating drug content in lornoxicam patches.

2.9.4. In vitro release study. The in vitro release profile of LRX from reservoir patches was determined by using USP Apparatus V (Paddle-over disk apparatus) (Erweka DT-600,

Heusenstamm, Germany). The vessels were filled with 500 mL of PBS pH 7.4 and the temperature was maintained at $32 \pm 0.2^\circ\text{C}$. The fabricated reservoir patches (30 cm^2) were sandwiched between a watch glass and a wire-screen (17-inch mesh) (Labex, Santa Clarita California, USA) and immersed into the dissolution medium. Aliquots of 5 ml were withdrawn and replaced with fresh medium at specified time points i.e. 0.5, 1, 2, 3, 4,5, 6, 7, 8, 9 and 10 h. The samples were suitably diluted and analyzed by means of a double beam UV-Spectrophotometer at 376 nm [22]. Each experiment was repeated in triplicate.

Various kinetic models were used to determine the release kinetics such as zero-order, first-order, Higuchi model Korsmeyer—Peppas model, Weibull and Makoid–Banakar model [23, 24]. The coefficient of correlation (R^2) and rate constants was determined using Excel Add-In Program DD Solver[®] [25] and values of R^2 were compared to determine the best-fitted model. The equations of models are as follows:

Zero-order:

$$Q_t = Q_o + k_o t \tag{2}$$

where Q_o and Q_t represent the initial amount of drug in dosage form and amount of drug at time t , respectively. k_o is a zero-order rate constant.

First—order:

$$\log Q_t = \log Q_o + \frac{k_1 t}{2.303} \tag{3}$$

Where k_1 is the first order rate constant.

Higuchi model:

$$Q_t = k_H t^{1/2} \tag{4}$$

Where k_H is the Higuchi rate constant.

Korsmeyer-Peppas model:

$$\frac{M_t}{M_\infty} = K t^n \tag{5}$$

Where, M_t/M_∞ is the fraction of the drug released at time t , K is rate constant and n is the release exponent indicating the drug release mechanism.

Weibull model:

$$m = 1 - \exp\left[\frac{-(t - T_l)^b}{a}\right] \tag{6}$$

Where ‘ m ’ is drug accumulated fraction in solution at any time t . The scale parameter is, a , defining time scale process. Lag time is presented by T_l i.e. the time required before the onset of drug release, in most cases, it will be zero. b is considered as a shape parameter and expresses curve.

Makoid-Banakar model:

$$\frac{M_t}{M_\infty} = k_{MB} t^n e^{(-ct)} \tag{7}$$

Where, K_{MB} , n , and c are empirical parameter (K_{MB} , n , $c > 0$) and M_t/M_∞ is the accumulation fraction of the drug in solution at time t .

2.9.5. In vitro permeation study. The skin of Wistar albino rats (150–180 g) was used for in vitro permeation studies. The rats were sacrificed by giving anesthesia (ether). The skin hair of animals was surgically removed with an electrical clipper. To remove adhering fat, the dermis side of the skin was wiped with isopropyl alcohol. After washing with PBS, the skin was enclosed in aluminum foil and stored in a deep freezer at -20°C until further use. Before the experiment, the skin was brought to room temperature and placed carefully in the vessel containing the dissolution medium.[26]

For in vitro permeation studies, Franz diffusion cell is commonly used equipment. However, reservoir patches with larger surface area can't be fitted into the donor chamber of its cell without cutting, which results in loss of patch integrity. Prodduturi et al. recommended the use of USP apparatus V for permeation studies of such patches. [27] Therefore, in the present study, USP apparatus V was used for permeation studies of LRX reservoir patches.

The vessel was filled with 600 mL of Hank's balanced salt solution. The sample patch was applied on the rat skin which was then adjusted between watch glass and wire screen and placed in the vessel. The temperature was maintained at $32 \pm 0.2^{\circ}\text{C}$ and the rotation of apparatus was adjusted at 100 rpm. Aliquots of 10 ml were withdrawn at 0.5, 1, 2, 3, 4, 5, 6, 7, 8, 9 and 10 h and were substituted with an equivalent volume of the medium. Each sample was diluted and analyzed using the HPLC mentioned above for determining the content uniformity of drug in patches [7]. Each experiment was performed in triplicate. The cumulative amount of drug permeated through rat skin was plotted against time for all the formulated patches. [28]

Flux (J , $\mu\text{g}/\text{cm}^2/\text{h}$) was determined from the slope of the linear portion of cumulative amount permeated per unit area vs time, and time lag (T_l) was determined by extrapolation of the line to the abscissa.[29]. The permeability coefficient (P) was calculated using Fick's First Law of diffusion which is described as

$$P = J/C_o \quad (8)$$

Where J is the steady-state permeation flux and C_o is the initial concentration.

The diffusion coefficient (DC) was calculated using the relation derived from Fick's second law of diffusion which is described in Eq 9:

$$DC = \frac{h^2}{6T_l} \quad (9)$$

Where T_l is the lag time and h is the thickness of the skin. [30]

The rate of drug delivery is either controlled by the device or stratum corneum. [31].The fraction rate controlled by the device (F_D) and skin (F_S) is computed by the following equations:

$$F_D = \frac{M_{total}}{M_{device}} \quad (10)$$

$$F_S = 1 - F_D \quad (11)$$

2.9.6. Evaluation of formulation factors. The impact of varying formulation factors such as concentration of carbopol (0.5%, 1%, 1.5%), drug loading concentrations (20 mg, 30 mg, 40 mg), surface area (20 cm^2 , 30 cm^2 , 40 cm^2), rate controlling membranes (3M Cotran-9728 and 3M CoTran-9716), adhesive DURO-TAK 387/2510 and different rpm (50, 75 and 100 rpm) on drug release and permeation of optimized transdermal reservoir patch was also investigated. For the evaluation of each factor, separate patches were developed as described previously.

2.10. Skin irritation study

The skin irritation studies were carried out according to the method described by Draize et al. [32] The animals were divided into three groups each containing six rats. Group I served as the control, group II was treated with optimized LRX patch while group III received 0.8% aqueous solution of formalin as the standard irritant. The rats were clipped free of hair 24 h before the experiment. The patches were applied on the rat skin and the application site was covered and wrapped with an elastic adhesive bandage. The skin reactions were evaluated in accordance with the Draize method. [33].

2.11 In vivo analgesic and anti-inflammatory activities

2.11.1. Hot-plate reaction time. The analgesic activity of LRX was performed by the Hot-plate Analgesic method. This method was reported by Baker et al [34] and was adopted with slight modifications for reservoir patches. Animals were divided into three groups (n = 6 for each group). Group I served as control, group II served as standard and received 4mg/kg LRX orally [35] and group III was treated with the optimized patch (4 cm²). The test patch was applied topically on the posterior paw of each rat of the treated group and the response time was recorded after 0, 30, 60, 120 and 180 min after application. Each rat was placed on a hot plate (MOD 39D Hot meter, Columbus, USA) maintained at 55 ± 1 °C and the latency period was recorded. The responses to pain stimulus include jumping/raising and licking of the hind foot. The animals were observed for any gross behaviour changes, morbidity and mortality.

2.11.2. Acetic acid-induced writhing response. Writhing induced by acetic acid was also used to assess the analgesic effect of LRX reservoir patch. Male Albino rats were divided into three groups (n = 6 for each group). The animals were weighed and numbered appropriately. Normal saline was given to the control group (Group I), the standard group (group II) received oral LRX (4 mg/kg) and the test group (group III) received an optimized LRX patch (4 cm²) prior to administration of acetic acid. The hair on the abdominal skin of rats was removed 12 h prior to the application of the patch. After 1 h of application, the patches were removed and acetic acid in the concentration of 1% was injected intraperitoneally to all groups. Five minutes later, the number of writhings (W) within 20 minutes was recorded. [36] The pain inhibition ratio (PIR) was calculated according to the following formula:

$$PIR = \frac{W_{blank} - W_{administration}}{W_{blank}} \quad (12)$$

2.11.3 Carrageenan hind paw edema test

The anti-inflammatory activity of LRX patches was evaluated through the Carrageenan-hind paw edema test reported by Winter et al in 1962 [37]. The method was adopted with slight modifications. The animals were divided into three groups, each comprising of six animals. Group I served as control (only carrageenan is administered). Group II was treated with oral LRX (4 mg/kg). Group III was treated with the optimized patch (4 cm²) which was applied topically on the left hind paw. The test patch was applied 1 h prior to the carrageenan injection. After 1 h, 0.1 mL of carrageenan solution (1%) was injected in the left hind paw of all groups. The paw edema was measured at 1, 2, 3, 4, 5 and 6 h using a Vernier caliper (Seiko brand, China). The percent inhibition of edema was calculated through the following equation:

$$\% \text{ edema Inhibition} = \frac{\%edema_{(control)} - \%edema_{(drug)}}{\%edema_{(control)}} \times 100 \quad (13)$$

2.11.4 Statistical analysis. For in vivo studies, the difference between control groups and treated groups was assessed by one-way ANOVA using Tukey's multiple comparison post-hoc test. A probability level of $P < 0.05$ was considered statistically significant. Statistical evaluations were performed by SPSS (Version 20).

2.12. Stability studies

Accelerated stability studies for the designed patches were performed by storing the replicates of LRX patches under three different temperature conditions i.e. at 4°C, room temperature and 45°C [38]. The samples were analyzed at an interval of 0, 30, 60 and 90 days for physical appearance and drug content determination. HPLC method was used for evaluating the drug content [7]. In vitro permeation study was also performed in triplicate for samples stored at 4°C.

Result and discussion

3.1 Solubility of lornoxicam

The solubility of a drug plays an important role in obtaining appropriate bioavailability. The main hindrance which comes across in the development of new drug molecules is low aqueous solubility. Most of the drugs are either weakly acidic or weakly basic and have poor aqueous solubility. Lornoxicam is also one of those drugs which exhibit poor aqueous solubility. The solubility studies for the selected drug was carried out in the water, Phosphate buffer pH 5.8, 6.8 and 7.4. According to the results, least solubility was observed in water i.e. 0.038 ± 0.001 mg/ml and the highest solubility was found in phosphate buffer pH 7.4 i.e. 0.346 ± 0.002 mg/ml. These results were parallel with the findings of Mundada et al where the solubility was highest in phosphate buffer 7.4 and was found to be 0.303 ± 0.008 mg/ml [2]

3.2 Characterization of gels

Table 2 represents the physicochemical characteristics of the formulated gels. All gels exhibited appropriate cosmetic qualities such as uniform color, homogeneity, smooth texture and no phase separation. The pH of gel formulations F1-F9 ranged between 6.25 ± 0.03 and 6.80 ± 0.045 . The pH values were found closer to 7, which is suitable for transdermal preparation [39]. The viscosity of the gels ranged between 1300 ± 0.83 cps and 5130 ± 0.59 cps and the drug content was found within specified limit i.e. 90–110%

Table 2. Physicochemical characterization of lornoxicam gels F1-F9 (n = 3).

Formulation Code	pH	Drug Content	Viscosity
		(%)	(cps)
F1	6.75 ± 0.07	100.46 ± 0.451	1300 ± 0.83
F2	6.25 ± 0.03	101 ± 0.152	5130 ± 0.59
F3	6.30 ± 0.04	100.2 ± 0.500	2850 ± 0.77
F4	6.55 ± 0.06	100.5 ± 0.65	3150 ± 0.34
F5	6.28 ± 0.03	98.45 ± 0.89	2250 ± 0.52
F6	6.42 ± 0.05	100.2 ± 0.79	3300 ± 0.75
F7	6.80 ± 0.045	96.75 ± 0.34	2500 ± 0.64
F8	6.41 ± 0.01	99.9 ± 0.46	2300 ± 0.53
F9	6.5 ± 0.05	100.45 ± 0.59	1750 ± 0.82

<https://doi.org/10.1371/journal.pone.0228908.t002>

3.3 Characterization of fabricated patches

The patches having a surface area of 30 cm² were developed and evaluated for weight, thickness, and content uniformity. The mean weight of reservoir patches F1-F9 was found to be 5.325 ± 0.008 g– 5.702 ± 0.105 g and thickness between 1.32 ± 0.005 mm– 1.435 ± 0.004 mm. The results indicate that there was a slight difference in the weight and thickness among the formulations. Content uniformity between $99.05 \pm 0.38\%$ and $100.54 \pm 0.12\%$ indicated good uniformity of drug content among all the formulations.

3.4 In vitro release study

An in vitro drug release evaluation experiment can give a reliable indication of the rate and extent of drug release from a transdermal patch. In reservoir-type transdermal patches, drug delivery is mainly governed by the release of drug from the patches.[40]. In such systems, there is an inherent secondary control due to its rate controlling membrane. Fig 1 represents the release profile which indicates maximum release from formulation F9 ($95.8 \pm 1.121\%$) followed by formulation F1 ($95.63 \pm 0.08\%$) in 10 h while formulations F2, F3 and F6 exhibited a release of less than 80%.

To study the release kinetics, data obtained from in-vitro drug release studies were plotted in various kinetic models which include zero order, first order, Higuchi, Korsmeyer-Peppas, Weibull and Makoid–Banakar. All the formulations best comply with Makoid–Banakar model showing R² values in the range of 0.998–0.999 as shown in Table 3. The reservoir patches of estradiol [22] and dexibuprofen[41]. have also followed the Makoid-Banakar model. When the 'c' value of the Makoid-Banakar model approaches zero, the model becomes identical to the Korsmeyer-Peppas model. [42]. The release exponent 'n' indicates the type of diffusion followed by the formulation. In the current study, n values were found between 0.5–1 showing Non-Fickian transport. [23]

3.5 In vitro permeation study

The permeation studies were carried out using whole rat skin. Full thickness abdominal skin was excised from Wistar albino rats and hair of the rats was removed with a clipper. Subcutaneous tissues, fats and tissues were also removed. The skin samples were cut into appropriate size for permeation studies. [7]. Fig 2 represents the permeation profile of formulated reservoir

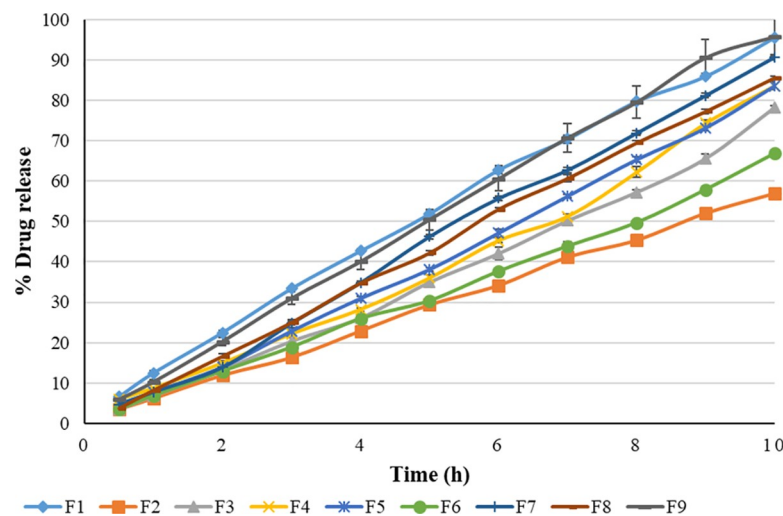


Fig 1. In vitro release profile of formulation F1-F9 (n = 3; mean ± SD) from lornoxicam reservoir patches.

<https://doi.org/10.1371/journal.pone.0228908.g001>

Table 3. Model fitting of the lornoxicam reservoir patches (F1-F9) release profile.

Mathematical models	F1	F2	F3	F4	F5	F6	F7	F8	F9
Zero-order									
R ²	0.996	0.992	0.989	0.987	0.991	0.994	0.995	0.99	0.998
k ₀ (h ⁻¹)	9.861	5.712	7.24	7.88	7.971	6.377	8.827	8.372	9.905
First-order									
R ²	0.947	0.967	0.928	0.9148	0.924	0.958	0.906	0.911	0.93
k ₁ (h ⁻¹)	0.167	0.074	0.101	0.114	0.116	0.086	0.135	0.124	0.167
Higuchi model									
R ²	0.877	0.813	0.794	0.7969	0.807	0.822	0.796	0.839	0.892
k _H (h ^{-1/2})	25.608	14.58	18.5	20.17	20.43	16.39	22.54	7.52	9.008
Korsmeyer-Peppas model									
R ²	0.995	0.997	0.996	0.9938	0.995	0.995	0.991	0.997	0.996
K _{kp} (h ⁻ⁿ)	12.198	4.9	5.369	5.985	6.471	5.717	6.729	6.25	10.793
n	0.894	0.774	0.938	0.836	0.873	0.954	0.934	0.945	0.959
Weibull									
R ²	0.985	0.997	0.984	0.975	0.98	0.987	0.989	0.99	0.986
T _d (h)	5.888	11.398	8.582	7.842	7.752	10.146	6.879	7.283	5.903
A	12.673	26.317	27.931	26.992	24.385	22.456	29.333	30.489	16.271
B	1.432	1.344	1.549	1.6	1.56	1.343	1.752	1.721	1.571
Makoid Banakar									
R ²	0.999	0.998	0.999	0.999	0.998	0.998	0.998	0.997	0.999
n	0.941	1.256	0.833	0.689	0.804	0.789	1.209	1.172	1.056
k _{MB}	11.86	4.299	6.696	8.184	7.949	6.801	6.37	6.124	10.132
c	0.008	0.03	-0.053	-0.075	-0.05	-0.046	0.012	0.004	0.017

<https://doi.org/10.1371/journal.pone.0228908.t003>

patches. The cumulative amount of LRX permeated per unit area from F1 and F9 was found to be 1179.2±6.87 µg/cm² and 1217.77±1.16 µg/cm², respectively. The permeation parameters were computed and presented in Table 4.

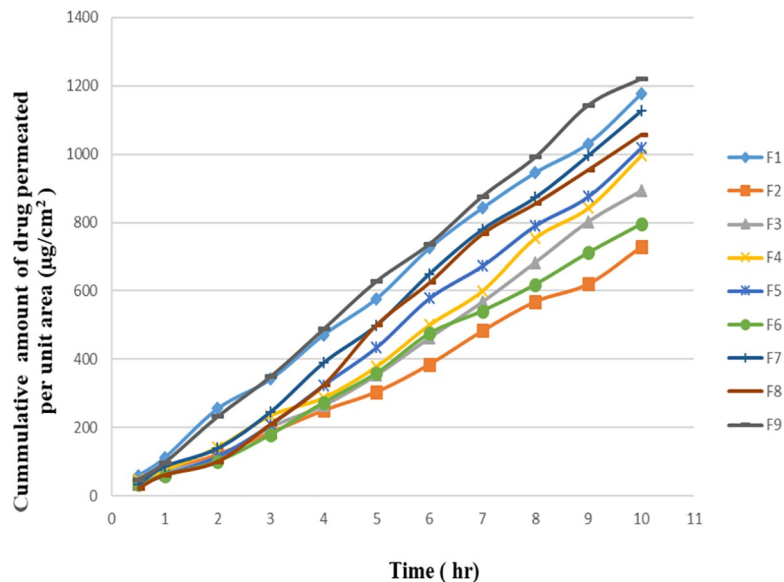


Fig 2. In vitro permeation profile of formulation F1-F9 (n = 3; mean ± SD) from lornoxicam reservoir patches.

<https://doi.org/10.1371/journal.pone.0228908.g002>

Table 4. Permeation parameters of lornoxicam reservoir patches (F1-F9).

Formulation code	Flux	Lag time	Permeability coefficient	Diffusion coefficient	F _D	F _S	Regression coefficient	Best fit equation for permeation plot
	(J)	(t _{lag})	(P)	(D)				
	µg/cm ² /h	H	cm/h	cm ² /h				
F1	122.52 ± 1.28	0.935 ± 0.29	3.06E-03	5.26E-05	0.923	0.077	0.9961	Q = 122.52t - 1.225
F2	67.74 ± 1.14	1.692 ± 0.09	1.69E-03	2.91E-05	0.911	0.089	0.9923	Q = 67.74t - 6.488
F3	93.56 ± 1.22	1.225 ± 0.24	2.33E-03	4.02E-05	0.862	0.138	0.9887	Q = 93.56t - 63.063
F4	101.50 ± 0.78	1.129 ± 0.26	2.53E-03	4.36E-05	0.905	0.095	0.9822	Q = 101.5t - 70.16
F5	106.29 ± 0.53	1.078 ± 0.45	2.65E-03	4.57E-05	0.929	0.07	0.9821	Q = 106.3t - 76.403
F6	80.28 ± 1.23	1.428 ± 0.38	2.00E-03	3.45E-05	0.888	0.112	0.9886	Q = 80.28t - 27.55
F7	117.42 ± 0.75	0.978 ± 0.12	2.93E-03	5.05E-05	0.973	0.027	0.9921	Q = 117.42t - 69.89
F8	115.98 ± 1.27	0.958 ± 0.43	2.89E-03	4.98E-05	0.914	0.086	0.988	Q = 115.99t - 94.20
F9	126.51 ± 1.19	0.908 ± 0.57	3.16E-03	5.43E-05	0.955	0.045	0.9986	Q = 126.51t - 22.768

<https://doi.org/10.1371/journal.pone.0228908.t004>

Almost 91.32% of the drug was permeated from formulation F9 in 10h with a maximum flux of 126.51 ± 1.19 µg/cm²/h and a minimum lag time of 0.908 ± 0.57h whereas, the permeability coefficient was found to be 3.16E-03 cm/h. In a study conducted by Yener et al, the permeation coefficient of the LRX transdermal patch was found to be 1.34E-3 cm/h in the presence of single penetration enhancer[43]. In another study, when OA and PG were used separately, the flux of LRX transdermal patches was found to be 17.97 ± 0.463 µg/cm²/h and 39.45 ± 0.74 µg/cm²/h, respectively.[44]. The results of the present study reveal that the presence of permeation enhancers as a cosolvent produces a significant impact on the permeation of LRX across the membrane. Similar results have been reported in previous studies where the combination of fatty acids and PG has produced significant enhancement on skin permeation rate of nifedipine, [45] physostigmine[46] and ketoprofen.[47].

Cosolvents have been widely used as vehicles as well as penetration enhancers in the transdermal formulation of drugs. In addition to affecting the drug solubility in the vehicle, cosolvents may alter the structure of the skin and modify the penetration rate. Thus, cosolvents can affect both drug release and percutaneous absorption. Moreover, the use of a cosolvent may offer synergistic enhancement. [12]

It has been revealed that there are separate hydrophilic and lipophilic domains present in the barrier area of the stratum corneum. Therefore, penetrants exhibiting both hydrophilic and lipophilic properties can probably penetrate stratum corneum more readily. Fatty acids are known to be enhancers with lipophilic properties and various studies have shown that the skin permeability enhancing effects of fatty acids are greater with PG. This binary system can disorganize the multilaminar hydrophilic-lipophilic layers located intercellularly in the stratum corneum, consequently promoting percutaneous absorption of drugs [48]

In the current investigation, it was observed that the presence of PG and OA has shown a good correlation between drug release and permeation of LRX. Maximum drug release (95%) and permeation (91.32%) can be achieved with this binary system of penetration enhancers. The drug release profile indicates a controlled release of LRX for 10h with a rate that is almost similar to that of the drug delivery rate through the rat skin. The F_D and F_S values were also calculated as shown in Table 4. The F_D values ranges from 0.862–0.955 for formulations F1-F9.

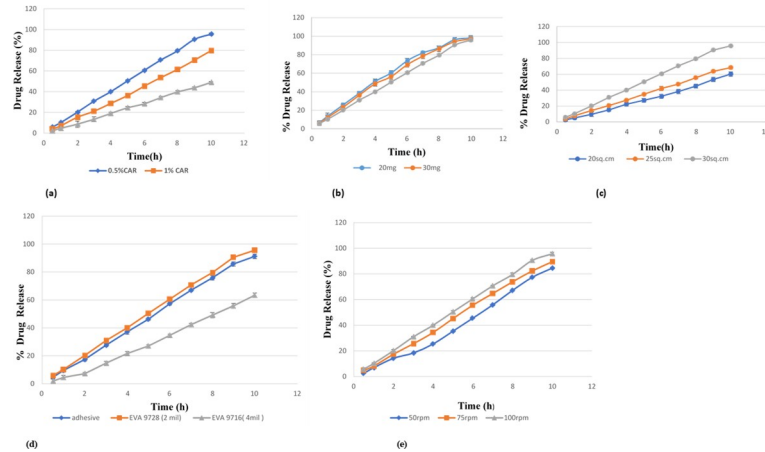


Fig 3. (a): Effect of gelling agent concentration on drug release. (b): Effect of drug loading on drug release. (c): Effect of surface area on drug release. (d): Effect of transdermal components on drug release. (e): Effect of agitation speed on drug release.

<https://doi.org/10.1371/journal.pone.0228908.g003>

Kalia and Guy [31] suggested that the value of F_d closer to 1 indicates that the device majorly controls drug permeation.

3.6 Effect of formulation factors

Different formulation factors such as gelling agent concentration, drug loading, surface area and rate controlling membrane were studied for drug release (Fig 3(A), 3(B), 3(C) and 3(D)) and drug permeation characteristics (Fig 4(A), 4(B), 4(C) and 4D)).

3.6.1 Effect of gelling agent concentration. The impact of varying concentration of gelling agent (0.5–1.5%) on release and permeation was investigated. It was observed that the increase in carbopol concentration has decreased the drug release and the rate of permeation across the skin as presented in Figs 3(A) and 4(A), respectively. This is similar to the findings of Patel et al. where an increase in the concentration of gelling agents leads to a significant decrease in drug release. [49]. This may be attributed to the increase in microviscosity of gel

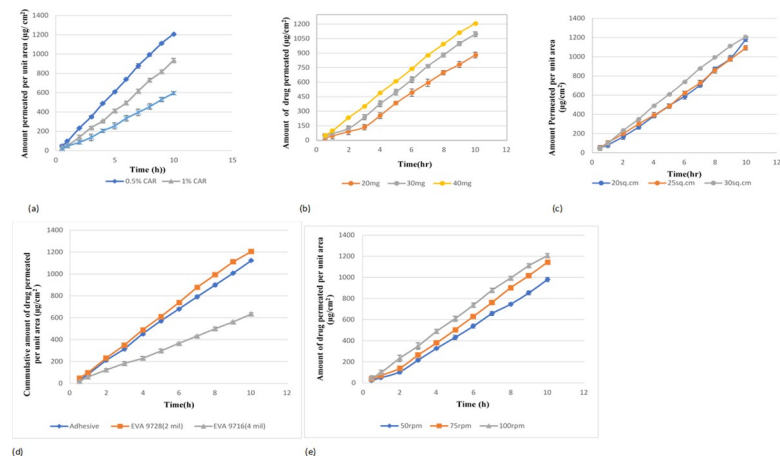


Fig 4. (a): Effect of gelling agent concentration on drug permeation. (b): Effect of drug loading on drug permeation. (c): Effect of surface area on drug permeation. (d): Effect of transdermal components on drug permeation. (e): Effect of agitation speed on drug permeation.

<https://doi.org/10.1371/journal.pone.0228908.g004>

leading to a decrease in the drug release and permeation. [50] The complex gel network has caused a longer diffusion pathway of the drug to be permeated through the membrane.

3.6.2 Effect of drug loading. The drug loading effect was evaluated by formulating patches containing varying quantities of LRX (20 mg, 30 mg, and 40 mg) and is presented in Figs 3(B) and 4(B). Lower drug loading leads to a faster release of the drug due to the formation of the drug enriched shell. [51] It was also observed in the current study, that the higher drug loading has significantly reduced the release of drug from patches. Whereas, flux has increased from $95.75 \mu\text{g}/\text{cm}^2/\text{h}$ to $126.51 \mu\text{g}/\text{cm}^2/\text{h}$ from the patches containing 20 mg and 40 mg drug, respectively. Similar results were reported in a study where high skin permeation of benzotropine was obtained with a higher drug loading in patch formulations. According to Fick's Law, skin permeation of a drug is usually proportional to the drug concentration when the drug concentration is below saturation. [52] There was good linearity between the skin permeation and the loading amount of Lornoxicam.

3.6.3 Effect of surface area. The surface area of the patch in contact with skin is the predictor of drug release. Patches of the variable surface area (20 cm^2 , 25 cm^2 and 30 cm^2) were also fabricated to evaluate the effect of surface area on drug release and permeation. Drug release at 20 cm^2 , 25 cm^2 and 30 cm^2 was found to be 60.27%, 68.41% and 95.8%, respectively. It was observed that drug release was dependent on the area of the devices as shown in Fig 3 (C). When the diameter of the device was increased, drug release was also increased. Thacharodi et al also concluded that the surface area of device affect the drug release and decrease in the area has also reduced the release of drug from the device [53]

Fig 4(C) represents drug permeation from LRX patches with different surface area and was found approximately similar i.e $115.58 \mu\text{g}/\text{cm}^2/\text{h}$, $110 \mu\text{g}/\text{cm}^2/\text{h}$ and $126.51 \mu\text{g}/\text{cm}^2/\text{h}$, respectively

Similar findings were reported by Ali et al, where a change in the surface area resulted in a different release profile but approximately similar permeation profile.[41].

3.6.4 Effect of rate-controlling membrane. The impact of rate-controlling membrane on drug release and permeation was also examined by using EVA membranes having variable vinyl acetate content i.e. 19% (3M CoTran-9728) and 9% (3M CoTran-9716). It was observed that the drug release and flux has increased with the increase in vinyl acetate content as shown in Figs 3(D) and 4(D). This may be attributed to the difference in vinyl acetate content in EVA membranes. These results were in accordance with Shin et al where the increase in vinyl acetate content resulted in increased drug release and permeation. [54]. Yang et al also reported the use of EVA membrane with 19% vinyl acetate content as a suitable controlled-release membrane for the development of transdermal reservoir patch of bufalin. [55]. Therefore, EVA membrane 9728 was selected for designing the optimized formulation.

3.6.5 Effect of adhesive. The selection of suitable pressure-sensitive adhesive is an important aspect of developing the transdermal delivery system[56]. Besides the drug itself, PSAs can also affect drug delivery from the developed patch. Therefore, the selection of an appropriate PSA is an important factor in designing a transdermal delivery system. In the current study, the effect of adhesive on drug release and permeation was evaluated using Duro-Tak 387/2510. The presence of carboxyl functional group in this adhesive contributes significantly to increase solubility and drug release[14] It has been reported that the use of Duro-Tak 387/2510 increases the permeation more as compared to other adhesives[57]. Figs 3(D) and 4(D) presents the release and permeation profile of membrane coated with adhesive and without adhesive. The drug release and permeation with adhesive was $91.24 \pm 1.2\%$ and $1122.59 \pm 4.13 \mu\text{g}/\text{cm}^2$ while without adhesive, the release and permeation were observed as $95.8 \pm 1.18\%$ and $1217.77 \pm 1.16 \mu\text{g}/\text{cm}^2$, respectively.

3.6.6 Effect of agitation speed. Figs 3(E) and 4(E) represent the impact of agitation speed on release and permeation. Minor variations in stirring rates don't impact the release profile

significantly [58]. This was also observed in the current study where variation in agitation speed lead to a slight difference in the release and permeation profiles. The release from lornoxicam patches agitated at 50 rpm, 75 rpm, and 100 rpm was found to be $84.5 \pm 0.46\%$, $89.46 \pm 0.55\%$ and $95.8 \pm 1.12\%$, respectively and flux was found to be $102.97 \mu\text{g}/\text{cm}^2/\text{h}$, $119 \mu\text{g}/\text{cm}^2/\text{h}$ and $126.51 \mu\text{g}/\text{cm}^2/\text{h}$, respectively.

3.7 Formulation optimization

3^2 Full factorial design was selected for the optimization of LRX patches. Two factors were evaluated each at 3 levels and experimental trials were carried out at all 9 possible combinations. PG (X_1) and OA (X_2) were selected as independent variables whereas dependent variables were Q_{10} (Y_1), flux (Y_2) and lag time (Y_3). A statistical model incorporating interactive and polynomial terms was used to evaluate the responses.

$$Y = b_0 + b_1X_1 + b_2X_2 + b_{12}X_1X_2 + b_{11}X_1^2 + b_{22}X_2^2 \quad (14)$$

Where Y represents the dependent variable, b_0 is the arithmetic mean response of the 9 runs, and b_i is the estimated coefficient for the factor X_i . The effects (X_1) and (X_2) indicate the average result of changing 1 factor at a time from its low to high value. The interaction terms (X_1X_2) describes the change in response when 2 factors are changed simultaneously. The polynomial terms (X_1^2) and (X_2^2) are added to observe nonlinearity. Data analysis was performed using Design-Expert 11 software (Stat ease, Minneapolis, MN)

The results clearly indicate that the drug release at 10^{th} h, flux and lag time were strongly dependent on the selected independent variables. The quadratic model was observed as the best-fitted model. Insignificant terms with $P > 0.05$ were removed to generate reduced models. However, the terms having $P < 0.05$ were considered statistically significant and were retained in the reduced models. Equations were developed for reduced quadratic models of Y_1 (Q_{10}), Y_2 (flux) and Y_3 (lag time) which are given as:

$$Y_1 = 90.06 + 8.67A - 8.51B - 12.19A^2 \quad (15)$$

$$Y_2 = 116.74 + 13.76A - 12.31B - 19.28A^2 \quad (16)$$

$$Y_3 = 0.99 - 0.19A + 0.16B + 0.25A^2 \quad (17)$$

The predicted values of formulations were also generated, Table 5 represents the comparative levels of experimental and predicted responses of different lornoxicam reservoir patches which suggests that the predicted values for Q_{10} (Y_1), flux (Y_2) and lag time (Y_3) were very close to that of experimental values. Table 6 describes the summary statistics for reduced quadratic models. The predicted R^2 values for responses Y_1 , Y_2 and Y_3 are in reasonable agreement with the adjusted R^2 .

The formulation F9 consisting of 0.5% carbopol, 10% PG and 3% OA was considered as the optimized formulation of LRX reservoir patch with Q_{10} (95.8%), flux ($124.9 \mu\text{g}/\text{cm}^2/\text{h}$) and lag time (0.918 h). Fig 5 represents contour plots and 3D response surface plots indicating that the maximum release, flux and minimum lag time were observed when mid-value of PG and OA were used.

3.8 Skin irritation study

Transdermal systems are intended for application on the skin, hence it is necessary to examine the biocompatibility of such formulations with the skin. The pressure sensitive adhesives used

Table 5. Comparison of experimental results (mean ± SD; n = 3) and predicted values.

Formulation code	Experimental responses			Predicted Responses		
	Q ₁₀ (%)	J (µg/cm ² /h)	t _{lag} (h)	Q ₁₀ (%)	J (µg/cm ² /h)	t _{lag} (h)
F1	95.63±1.12	122.52± 1.28	0.935±0.29	95.51	123.53	0.89
F2	57.01±0.40	67.74± 1.14	1.692±0.09	60.66	71.39	1.59
F3	78.34±0.53	93.56± 1.22	1.225±0.24	78.06	96.68	1.21
F4	83.69±0.83	101.50± 0.78	1.129±0.26	82.74	98.01	1.19
F5	83.66±0.96	106.29± 0.53	1.078 ± 0.45	81.47	104.43	1.15
F6	66.91±0.66	80.28 ± 1.23	1.428± 0.38	69.2	83.7	1.45
F7	90.73±0.62	117.42± 0.75	0.978± 0.12	91.55	118.19	0.93
F8	85.65±0.38	115.98± 1.27	0.958 ± 0.43	86.6	112.22	1.05
F9	95.8±0.08	126.51± 1.19	0.908 ± 0.57	95.54	121.73	0.93

<https://doi.org/10.1371/journal.pone.0228908.t005>

for adhering the patch may produce skin reactions. Therefore, skin irritation study is essential to examine the skin sensitivity to the applied patches[59]. The results obtained for skin irritation study showed satisfactory results as shown in Table 7. According to Draize et al, compounds that produce scores of 2 or less are considered negative i.e. no skin irritation. [32]. Hence, the fabricated LRX patch was declared safe for use.

3.9 In vivo analgesic and anti-inflammatory activities

3.9.1 Hot-plate test. In order to evaluate the analgesic efficacy of the formulated LRX reservoir patches, Hot-plate studies were carried out using Wister albino rats. The analgesic activity of Lornoxicam patch was manifested by their resistance or tolerability to the sensation of heat until licking their paws or jumping. Findings from this study demonstrated that the newly formulated LRX patch exhibited significant analgesic effect against thermal pain stimuli as shown in Table 8. Similar results were demonstrated by Baviskar et al where the matrix-type lornoxicam patches exhibited potent analgesic effect against thermal pain stimuli.[35]. Statistically, a significant difference was observed (P < 0.01) in the reaction time between the test and control group. However, the difference between the reaction time of the test and the standard group was found to be insignificant (P > 0.05).

3.9.2 Acetic acid induced writhing response. Acetic acid-induced writhing method was also adopted for the evaluation of the analgesic activity. Writhing is defined as a stretch, tension to one side, extension of hind legs, contraction of the abdomen so that the abdomen of mice touches the floor, turning of the trunk (twist). Any writhing is considered as a positive response[60] In order to assess the analgesic effect of the drug, it is considered as highly sensitive and useful method. The current study reveals that the test and standard drug significantly (P < 0.01) reduces the number of abdominal constrictions and stretching of hind limb induce

Table 6. Model summary statistics (for reduced quadratic model).

Responses	PRESS	R ²	Adjusted R ²	Predicted R ²	Adequate precision	SD	%CV	F-value	P-value	Comments
									Prob>F	
Y ₁	543.37	0.987	0.9845	0.9843	10.253	5.56	6.55	12.85	0.0086	significant
Y ₂	927.66	0.9042	0.9038	0.9035	11.317	7.35	7.05	15.52	0.0054	significant
Y ₃	0.16	0.981	0.9095	0.9093	9.89	0.092	8.47	12.25	0.0099	significant

Values of “Prob > F” less than 0.0500 indicate model terms are significant. Values greater than 0.1000 indicate the model terms are not significant. Model reduction has been done to improve the model.

<https://doi.org/10.1371/journal.pone.0228908.t006>

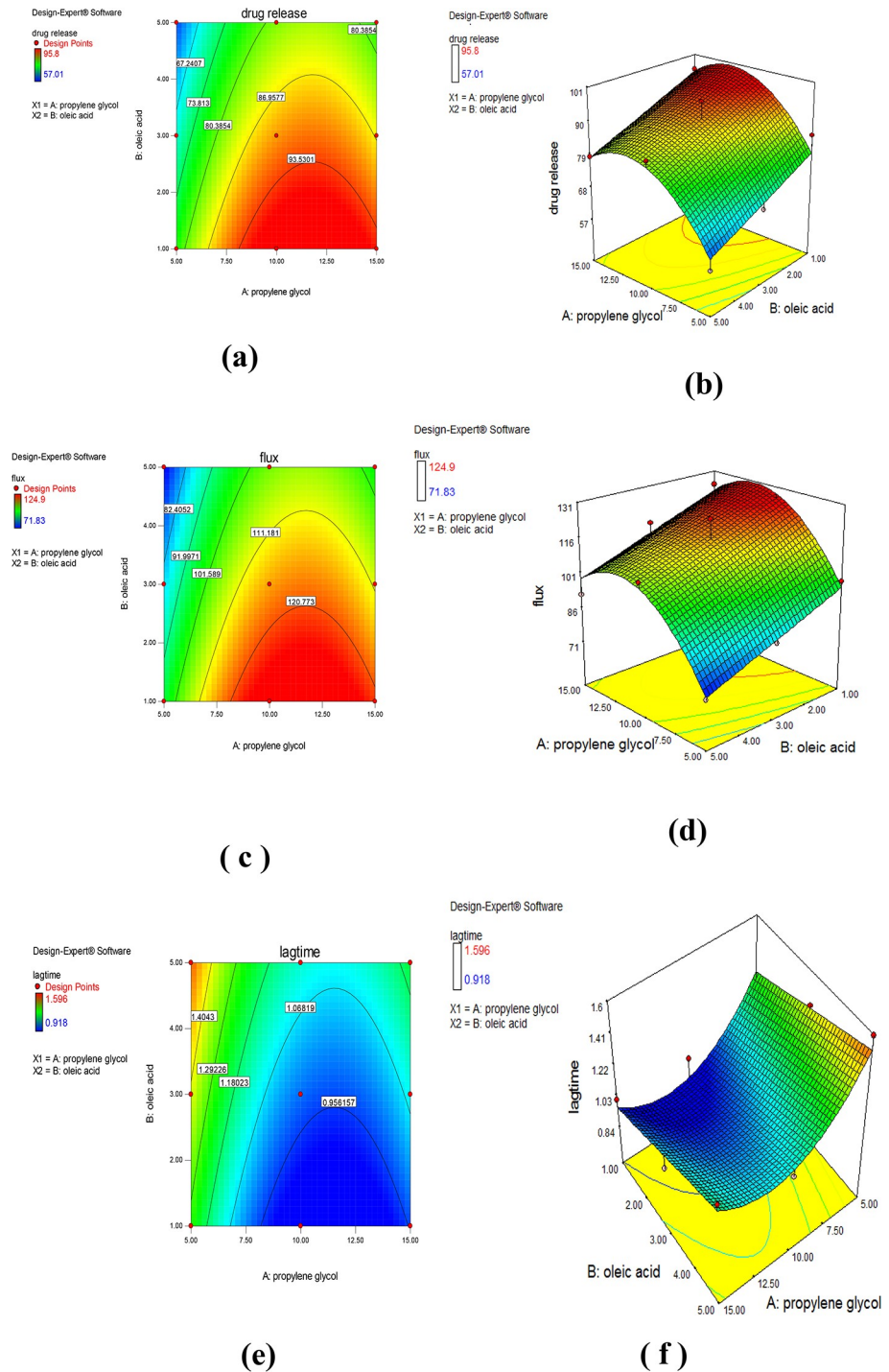


Fig 5. Contour plots (a) Q_{10} (c) Flux (e) Lag-time and responses surface curves (b) Q_{10} (d) Flux (f) Lag-time for optimization of lornoxicam reservoir patches.

<https://doi.org/10.1371/journal.pone.0228908.g005>

by the injection of Acetic acid as presented in Table 9. The selected formulation was also compared to the standard and the difference between them was found to be insignificant ($P > 0.05$).

In general acetic acid causes pain by liberating endogenous substances such as serotonin histamine, prostaglandins, bradykinins.[61] The significant increase in pain threshold by test

Table 7. Skin irritation study of optimized lornoxicam reservoir patch (mean ± SD; n = 6).

Rat No.	Control		F9		Formalin	
	Erythema ^a	Edema ^b	Erythema ^a	Edema ^b	Erythema ^a	Edema ^b
1	0	0	1	0	3	2
2	0	0	2	1	2	3
3	0	0	0	1	3	1
4	0	0	1	0	2	2
5	0	0	2	2	2	3
6	0	0	1	0	2	2
Average	0	0	1.16 ± 0.752**	0.66 ± 0.816**	2.333 ± 0.516	2.166 ± 0.752

**p<0.01, significant when compared to formalin

a: Erythema scale: score 0, no erythema; score 1: very slight erythema; score 2: well defined erythema; score 3: moderate to severe erythema; and score 4: severe erythema and scar formation.

b: Edema scale: score 0: no edema; score 1: very slight edema; score 2: slight edema; score 3: moderate edema; and score 4: severe edema

<https://doi.org/10.1371/journal.pone.0228908.t007>

and standard in these models suggests inhibition of PGs, Leukotrienes and other endogenous substances which are mainly responsible for producing pain.

3.9.3 Carrageenan hind-paw edema test. Carrageenan-induced rat paw edema is a commonly used model for studying the anti-inflammatory effect of drugs in rats. Carrageenan induces inflammation that is acute, non-immune and reproducible, which is characterized by an increase in the size of hind paw[62].

In the present investigation, the swelling in the paw size of rats was observed for 6h and % inhibition was calculated. As shown in Fig 6, there is a significant difference (P<0.001) in the swelling of paw size between control and test group. However, no significant difference (P>0.05) was observed between orally administered LRX and test group. The percent inhibition of edema is also represented graphically indicating a significant reduction in hind paw swelling after application of test patch followed by orally administered lornoxicam. These results were in good agreement with Nabarawi et al where both oral and transdermal groups showed increased inhibition than the control group.[44]

Smith et al [63] reported that NSAIDs mainly produce their effect by inhibition of COX enzymes. COX exists in two isomeric forms as COX 1and COX 2. LRX was found to be a potent inhibitor of COX1 and COX 2 and produce marked analgesic and anti-inflammatory effects.

LX is at least 10 times more potent as an antiinflammatory agent than piroxicam and was also tenfold more active than tenoxicam in inhibiting carrageenan-induced edema in the rat paw swelling in the adjuvant-induced polyarthritic rat [64]

Table 8. Analgesic effect of optimized lornoxicam reservoir patch on the reaction time of rats by hot plate method (mean ± SD; n = 6).

Group	Treatment	Reaction time in seconds									
		Paw licking					Jump Response				
		0 min	30 min	60 min	120 min	180 min	0 min	30 min	60 min	120 min	180 min
I	Control	35.5 ± 0.4	38.2 ± 0.3	38.8 ± 0.6	36.3 ± 0.5	38.4 ± 0.4	74.2 ± 0.8	75.4 ± 1.2	75.8 ± 0.9	74.3 ± 1.1	75.2 ± 0.5
II	Standard	37.5 ± 0.5	43.4 ± 0.7**	50.2 ± 0.4**	55.4 ± 0.7**	60 ± 0.5**	76.3 ± 0.7	82 ± 0.6**	88.4 ± 0.4**	95 ± 0.6**	103 ± 0.9**
III	Test	36.3 ± 0.24	44.5 ± 0.6**	49.22 ± 0.52**	53.35 ± 0.25**	58.88 ± 0.74**	74.35 ± 0.55	84.4 ± 0.56**	89.5 ± 0.3**	94 ± 0.4**	101 ± 0.6**

**P<0.01, significantly different from control (Tukey’s multiple comparison post-hoc test)

<https://doi.org/10.1371/journal.pone.0228908.t008>

Table 9. Effect of optimized lornoxicam formulation on 1% acetic acid induced writhes in the rat model (mean ± SD; n = 6).

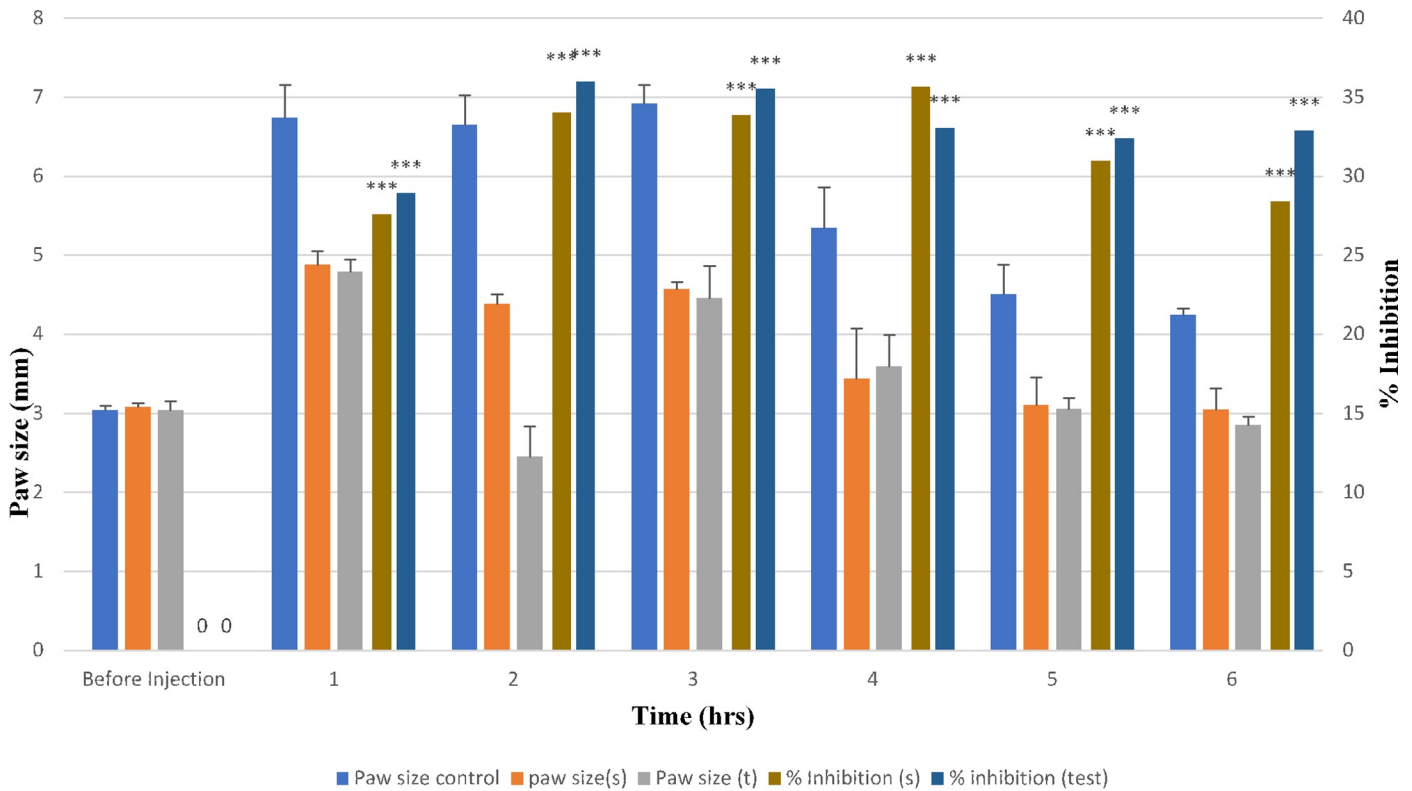
Group	Treatment	Writhes (n)	%age inhibition of Writhes
I	Control	16 ± 0.57	-
II	Standard	8.5 ± 0.28**	46.87
III	Test	10 ± 0.15**	37.5

**P<0.01 significantly different from control (Tukey’s multiple comparison post -hoc test).

<https://doi.org/10.1371/journal.pone.0228908.t009>

3.10 Stability studies

The stability testing of LRX patch was carried out at 4°C, room temperature, and 45°C over a period of 3 months. Fig 7(A) represents the LRX content in the patch after 3 months, which was found to be 95.79 ± 1.80%, 93.75 ± 2.24% and 90.50 ± 1.55% when kept at 4°C, room temperature, and 45°C, respectively. It was observed that drug content was most affected at a higher temperature. Though potency loses at a higher temperature, no other interference was observed for other components in the patch. There was no extra peak in the chromatogram. Similar results had been reported by Kusum et al. [65]



***P < 0.001 compared to control (one – way ANOVA followed by Tukey’s multiple comparison post-hoc test).

Fig 6. Graphical presentation of anti-inflammatory activity of optimized lornoxicam reservoir patch; swelling of hind paw of control, standard and test rats (n = 6; mean ± SD) and % inhibition of standard and test.

<https://doi.org/10.1371/journal.pone.0228908.g006>

The shelf-life for LRX patches was also calculated and was found to be 196 days at 4°C, 140 days at room temperature and 131 days at 45°C. Thus, it is suggested to store the patches in the refrigerator due to their prolonged shelf life at low temperatures.

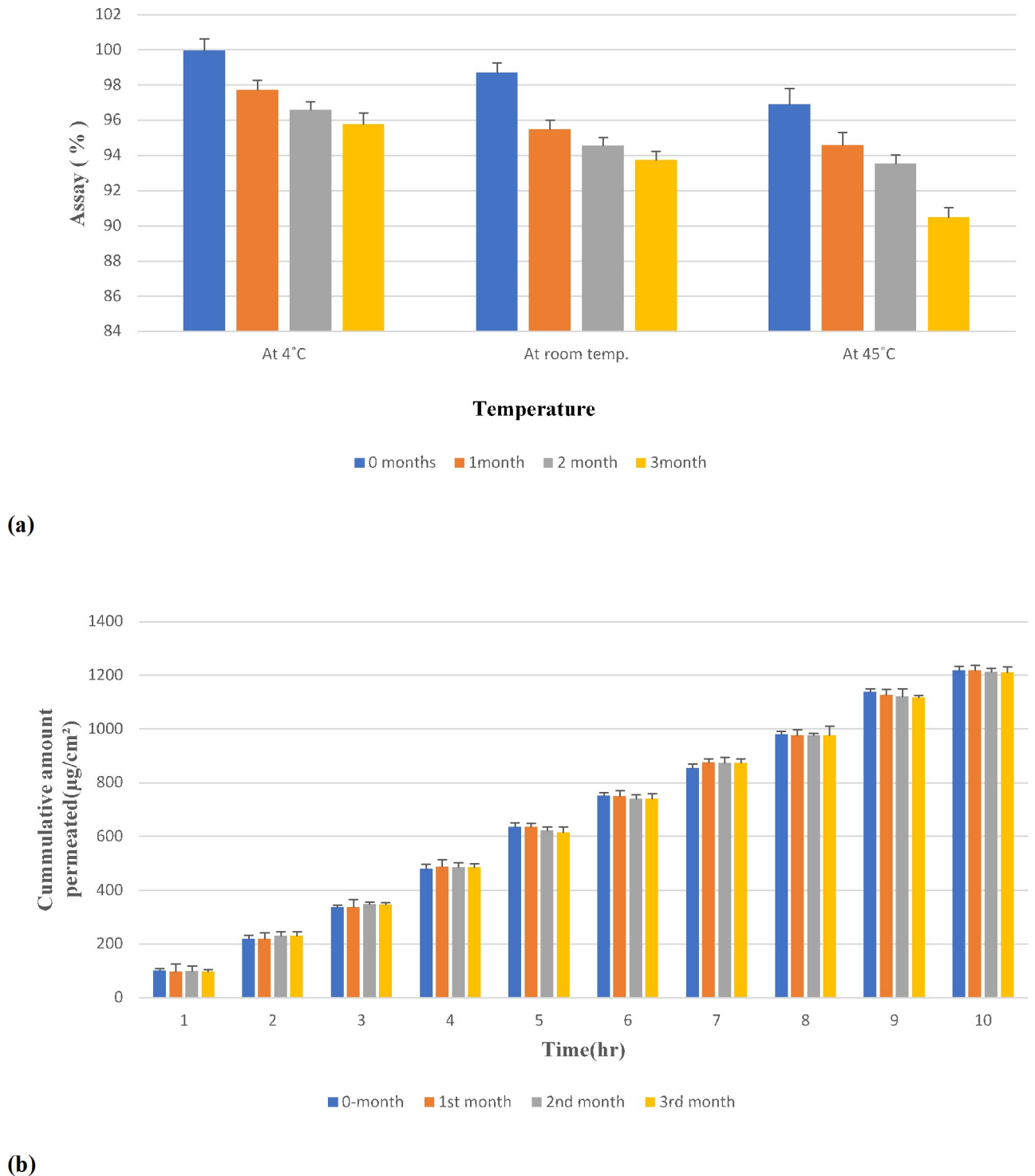


Fig 7. (a): Stability profile of lornoxicam reservoir patch at different temperatures. **(b):** Stability comparison profile of permeation (0–3 months) of lornoxicam patch at 4°C.

<https://doi.org/10.1371/journal.pone.0228908.g007>

In reservoir systems, the absorption of permeation enhancers by polymers of the membrane may lead to failure in the permeation of drugs across the skin.[66] The integrity of penetration enhancers was evaluated through the determination of transdermal permeation across rat skin. The results presented in Fig 7(B) show that drug permeation did not alter after three months when patches were stored at 4°C indicating the persistence in the integrity of penetration enhancers.

Conclusions

The membrane-based transdermal patches of LRX gel exhibiting controlled release was formulated. The use of OA and PG co-solvent as penetration enhancer were found effective in improving the flux of drug through the skin. The developed reservoir patches resulted in suitable analgesic and anti-inflammatory activity with no observed skin irritation. Thus, by achieving an effective therapeutic level of LRX with improved patient compliance, reduced gastrointestinal side-effects and dosing frequency, these transdermal patches can be used as an alternative to oral administration of Lornoxicam.

Supporting information

S1 Data.
(ZIP)

Author Contributions

Conceptualization: Muhammad Harris Shoaib.

Formal analysis: Durriya Hashmat.

Investigation: Durriya Hashmat.

Methodology: Fatima Ramzan Ali.

Supervision: Muhammad Harris Shoaib.

Validation: Fahad Siddiqui.

Writing – original draft: Durriya Hashmat.

Writing – review & editing: Muhammad Harris Shoaib.

References

1. Beetge E, du Plessis J, Müller DG, Goosen C, van Rensburg FJ. The influence of the physicochemical characteristics and pharmacokinetic properties of selected NSAID's on their transdermal absorption. *International journal of Pharmaceutics*. 2000; 193(2):261–4. [https://doi.org/10.1016/s0378-5173\(99\)00340-3](https://doi.org/10.1016/s0378-5173(99)00340-3) PMID: 10606790
2. Mundada M, Wankhede S, Patwardhan S, Avachat A. Formulation and evaluation of topical gel of lornoxicam using a range of penetration enhancers. *Indian J Pharm Edu Res*. 2012; 47:168–71.
3. Allen L, Ansel HC. *Ansel's pharmaceutical dosage forms and drug delivery systems*: Lippincott Williams & Wilkins; 2013.
4. Kumar R, Philip A. Modified transdermal technologies: Breaking the barriers of drug permeation via the skin. *Tropical Journal of Pharmaceutical Research*. 2007; 6(1):633–44.
5. Shinde AJ, Shinde AL, More HN. Design and evaluation of transdermal drug delivery system of gliclazide. *Asian Journal of Pharmaceutics (AJP)*: Free full text articles from Asian J Pharm. 2014; 4(2).
6. Chaudhary H, Rohilla A, Rathee P, Kumar V. Optimization and formulation design of carbopol loaded Piroxicam gel using novel penetration enhancers. *International journal of biological macromolecules*. 2013; 55:246–53. <https://doi.org/10.1016/j.ijbiomac.2013.01.015> PMID: 23376559

7. Gönüllü Ü, Üner M, Yener G, FATMA KARAMAN E, Aydoğmuş Z. Formulation and characterization of solid lipid nanoparticles, nanostructured lipid carriers and nanoemulsion of lornoxicam for transdermal delivery. *Acta Pharmaceutica*. 2015; 65(1):1–13. <https://doi.org/10.1515/acph-2015-0009> PMID: 25781700
8. Palei NN, Mohanta BC, Das MK, Sabapathi ML. Lornoxicam loaded nanostructured lipid carriers for topical delivery: Optimization, skin uptake and in vivo studies. *Journal of Drug Delivery Science and Technology*. 2017; 39:490–500.
9. Williams AC, Barry BW. Penetration enhancers. *Advanced drug delivery reviews*. 2012; 64:128–37.
10. Mittal A, Sara US, Ali A, Mohammed A. Design, development, physicochemical, in vitro and in vivo evaluation of monolithic matrix type transdermal patches containing nitrendipine. *Pharmaceutical development and technology*. 2009; 14(4):422–34. <https://doi.org/10.1080/10837450902748388> PMID: 19630699
11. Karande P, Mitragotri S. Enhancement of transdermal drug delivery via synergistic action of chemicals. *Biochimica et Biophysica Acta (BBA)-Biomembranes*. 2009; 1788(11):2362–73.
12. Arellano A, Santoyo S, Martin C, Ygartua P. Influence of propylene glycol and isopropyl myristate on the in vitro percutaneous penetration of diclofenac sodium from carbopol gels. *European journal of pharmaceutical sciences*. 1999; 7(2):129–35. [https://doi.org/10.1016/s0928-0987\(98\)00010-4](https://doi.org/10.1016/s0928-0987(98)00010-4) PMID: 9845796
13. Walters KA, Hadgraft J. *Pharmaceutical skin penetration enhancement: Informa Health Care*; 1993.
14. Gwak HS, Chun K. In vitro percutaneous absorption of tenoxicam from pressure-sensitive adhesive matrices across the hairless mouse skin. *Archives of pharmacal research*. 2001; 24(6):578–83. <https://doi.org/10.1007/bf02975169> PMID: 11794539
15. Al-Suwayeh SA, Taha EI, Al-Qahtani FM, Ahmed MO, Badran MM. Evaluation of skin permeation and analgesic activity effects of carbopol lornoxicam topical gels containing penetration enhancer. *The Scientific World Journal*. 2014;2014.
16. Dave BS, Amin AF, Patel MM. Gastroretentive drug delivery system of ranitidine hydrochloride: formulation and in vitro evaluation. *Aaps PharmSciTech*. 2004; 5(2):77–82.
17. Baker RW. *Controlled release of biologically active agents: John Wiley & Sons*; 1987.
18. Ahmed MO, Al-Badr AA. Lornoxicam. *Profiles of Drug Substances, Excipients and Related Methodology*. 36: Elsevier; 2011. p. 205–39.
19. Kim M-K, Zhao H, Lee C-H, Kim D-D. Formulation of a reservoir-type testosterone transdermal delivery system. *International journal of pharmaceutics*. 2001; 219(1–2):51–9. [https://doi.org/10.1016/s0378-5173\(01\)00631-7](https://doi.org/10.1016/s0378-5173(01)00631-7) PMID: 11337165
20. Zhan X, Mao Z, Chen S, Chen S, Wang L. Formulation and evaluation of transdermal drug-delivery system of isosorbide dinitrate. *Brazilian Journal of Pharmaceutical Sciences*. 2015; 51(2):373–82.
21. El Nabarawy NA, Abd Elmonem RA, Abo Enin HA. Development of economic transdermal patches containing lornoxicam for treatment of acute and chronic inflammatory models in albino rats (a preclinical study). 2014.
22. Costa P, Sousa Lobo J. Evaluation of mathematical models describing drug release from estradiol transdermal systems. *Drug development and industrial pharmacy*. 2003; 29(1):89–97. <https://doi.org/10.1081/ddc-120016687> PMID: 12602496
23. Costa P, Lobo JMS. Modeling and comparison of dissolution profiles. *European journal of pharmaceutical sciences*. 2001; 13(2):123–33. [https://doi.org/10.1016/s0928-0987\(01\)00095-1](https://doi.org/10.1016/s0928-0987(01)00095-1) PMID: 11297896
24. Singh B, Chauhan G, Sharma D, Kant A, Gupta I, Chauhan N. The release dynamics of model drugs from the psyllium and N-hydroxymethylacrylamide based hydrogels. *International journal of pharmaceutics*. 2006; 325(1–2):15–25. <https://doi.org/10.1016/j.ijpharm.2006.06.007> PMID: 16844329
25. Zhang Y, Huo M, Zhou J, Zou A, Li W, Yao C, et al. DDSolver: an add-in program for modeling and comparison of drug dissolution profiles. *The AAPS journal*. 2010; 12(3):263–71. <https://doi.org/10.1208/s12248-010-9185-1> PMID: 20373062
26. Ahad A, Aqil M, Kohli K, Sultana Y, Mujeeb M. Design, formulation and optimization of valsartan transdermal gel containing iso-eucalyptol as novel permeation enhancer: preclinical assessment of pharmacokinetics in Wistar albino rats. *Expert opinion on drug delivery*. 2014; 11(8):1149–62. <https://doi.org/10.1517/17425247.2014.914027> PMID: 24830648
27. Prodduturi S, Smith GJ, Wokovich AM, Doub WH, Westenberger BJ, Buhse L. Reservoir based fentanyl transdermal drug delivery systems: effect of patch age on drug release and skin permeation. *Pharmaceutical research*. 2009; 26(6):1344–52. <https://doi.org/10.1007/s11095-009-9843-0> PMID: 19229594
28. Hwang B-Y, Jung B-H, Chung S-J, Lee M-H, Shim C-K. In vitro skin permeation of nicotine from proliposomes. *Journal of controlled release*. 1997; 49(2–3):177–84.

29. Shahzad Y, Khan Q, Hussain T, Shah SNH. Influence of cellulose derivative and ethylene glycol on optimization of lornoxicam transdermal formulation. *International journal of biological macromolecules*. 2013; 61:26–32. <https://doi.org/10.1016/j.ijbiomac.2013.06.049> PMID: 23827761
30. Panigrahi L, Pattnaik S, Ghosal SK. The effect of pH and organic ester penetration enhancers on skin permeation kinetics of terbutaline sulfate from pseudolatex-type transdermal delivery systems through mouse and human cadaver skins. *Aaps Pharmscitech*. 2005; 6(2):E167–E73. <https://doi.org/10.1208/pt060225> PMID: 16353974
31. Kalia YN, Guy RH. Modeling transdermal drug release. *Advanced drug delivery reviews*. 2001; 48(2–3):159–72. [https://doi.org/10.1016/s0169-409x\(01\)00113-2](https://doi.org/10.1016/s0169-409x(01)00113-2) PMID: 11369080
32. Draize JH, Woodard G, Calvery HO. Methods for the study of irritation and toxicity of substances applied topically to the skin and mucous membranes. *Journal of pharmacology and Experimental Therapeutics*. 1944; 82(3):377–90.
33. Aggarwal G, Dhawan S, Harikumar S. Formulation, in vitro, and in vivo evaluation of matrix-type transdermal patches containing olanzapine. *Pharmaceutical development and technology*. 2013; 18(4):916–25. <https://doi.org/10.3109/10837450.2011.609993> PMID: 21913873
34. Baker AK, Hoffmann VL, Meert TF. Dextromethorphan and ketamine potentiate the antinociceptive effects of μ -but not δ - or κ -opioid agonists in a mouse model of acute pain. *Pharmacology Biochemistry and Behavior*. 2002; 74(1):73–86.
35. Baviskar DT, Parik VB, Jain DJ. Development of Matrix-type transdermal delivery of lornoxicam: in vitro evaluation and pharmacodynamic and pharmacokinetic studies in albino rats. *PDA journal of pharmaceutical science and technology*. 2013; 67(1):9–22. <https://doi.org/10.5731/pdajpst.2013.00898> PMID: 23385560
36. Zhang Y, Cun D, Kong X, Fang L. Design and evaluation of a novel transdermal patch containing diclofenac and teriflunomide for rheumatoid arthritis therapy. *asian journal of pharmaceutical sciences*. 2014; 9(5):251–9.
37. Winter CA, Risley EA, Nuss GW. Carrageenin-induced edema in hind paw of the rat as an assay for antiinflammatory drugs. *Proceedings of the society for experimental biology and medicine*. 1962; 111(3):544–7.
38. Pichayakorn W, Suksaeree J, Boonme P, Taweepreda W, Amnuait T, Ritthidej GC. Deproteinised natural rubber used as a controlling layer membrane in reservoir-type nicotine transdermal patches. *Chemical engineering research and design*. 2013; 91(3):520–9.
39. Alves MP, Scarrone AL, Santos M, Pohlmann AR, Guterres SS. Human skin penetration and distribution of nimesulide from hydrophilic gels containing nanocarriers. *International journal of pharmaceutics*. 2007; 341(1–2):215–20. <https://doi.org/10.1016/j.ijpharm.2007.03.031> PMID: 17482392
40. Prausnitz MR, Mitragotri S, Langer R. Current status and future potential of transdermal drug delivery. *Nature reviews Drug discovery*. 2004; 3(2):115. <https://doi.org/10.1038/nrd1304> PMID: 15040576
41. Ali FR, Shoaib MH, Yousuf RI, Ali SA, Imtiaz MS, Bashir L, et al. Design, development, and optimization of dexibuprofen microemulsion based transdermal reservoir patches for controlled drug delivery. *BioMed research international*. 2017; 2017.
42. Al-Achi A, Gupta MR, Stagner WC. *Integrated pharmaceuticals: applied preformulation, product design, and regulatory science*: John Wiley & Sons; 2013.
43. Yener G, Üner M, Gönüllü Ü, Yildirim S, Kiliç P, Aslan SS, et al. Design of meloxicam and lornoxicam transdermal patches: Preparation, physical characterization, ex vivo and in vivo studies. *Chemical and Pharmaceutical Bulletin*. 2010; 58(11):1466–73. <https://doi.org/10.1248/cpb.58.1466> PMID: 21048338
44. El-Nabarawi MA, Shaker DS, Attia DA, Hamed SA. In vitro skin permeation and biological evaluation of lornoxicam monolithic transdermal patches. *Int J of Pharmacy and Pharm Sci*. 2013; 5(2):242–8.
45. Aboofazeli R, Zia H, Needham TE. Transdermal delivery of nicardipine: an approach to in vitro permeation enhancement. *Drug Delivery*. 2002; 9(4):239–47. <https://doi.org/10.1080/10717540260397855> PMID: 12511202
46. Wang MY, Yang YY, Heng PWS. Skin permeation of physostigmine from fatty acids-based formulations: evaluating the choice of solvent. *International journal of pharmaceutics*. 2005; 290(1–2):25–36. <https://doi.org/10.1016/j.ijpharm.2004.10.027> PMID: 15664127
47. Bowen JL, Heard CM. Film drying and complexation effects in the simultaneous skin permeation of ketoprofen and propylene glycol from simple gel formulations. *International journal of pharmaceutics*. 2006; 307(2):251–7. <https://doi.org/10.1016/j.ijpharm.2005.10.014> PMID: 16289881
48. Gwak HS, Oh IS, Chun IK. Transdermal delivery of ondansetron hydrochloride: effects of vehicles and penetration enhancers. *Drug development and industrial pharmacy*. 2004; 30(2):187–94. <https://doi.org/10.1081/ddc-120028714> PMID: 15089053

49. Patel J, Patel B, Banwait H, Parmar K, Patel M. Formulation and evaluation of topical aceclofenac gel using different gelling agent. *Int J Drug Dev Res*. 2011; 3(1):156–64.
50. Welin-Berger K, Neelissen JA, Bergenstahl B. The effect of rheological behaviour of a topical anaesthetic formulation on the release and permeation rates of the active compound. *European journal of pharmaceutical sciences*. 2001; 13(3):309–18. [https://doi.org/10.1016/s0928-0987\(01\)00118-x](https://doi.org/10.1016/s0928-0987(01)00118-x) PMID: 11384854
51. Wissing S, Müller R. Solid lipid nanoparticles as carrier for sunscreens: in vitro release and in vivo skin penetration. *Journal of Controlled Release*. 2002; 81(3):225–33. [https://doi.org/10.1016/s0168-3659\(02\)00056-1](https://doi.org/10.1016/s0168-3659(02)00056-1) PMID: 12044563
52. Hai NT, Kim J, Park E-S, Chi S-C. Formulation and biopharmaceutical evaluation of transdermal patch containing benzotropine. *International journal of pharmaceutics*. 2008; 357(1–2):55–60. <https://doi.org/10.1016/j.ijpharm.2008.01.024> PMID: 18417307
53. Thacharodi D, Rao KP. Development and in vitro evaluation of chitosan-based transdermal drug delivery systems for the controlled delivery of propranolol hydrochloride. *Biomaterials*. 1995; 16(2):145–8. [https://doi.org/10.1016/0142-9612\(95\)98278-m](https://doi.org/10.1016/0142-9612(95)98278-m) PMID: 7734649
54. Shin S-C, Lee H-J. Controlled release of triprolidine using ethylene-vinyl acetate membrane and matrix systems. *European journal of pharmaceutics and biopharmaceutics*. 2002; 54(2):201–6. [https://doi.org/10.1016/s0939-6411\(02\)00051-6](https://doi.org/10.1016/s0939-6411(02)00051-6) PMID: 12191692
55. Yang Z, Teng Y, Wang H, Hou H. Enhancement of skin permeation of bufalin by limonene via reservoir type transdermal patch: formulation design and biopharmaceutical evaluation. *International journal of pharmaceutics*. 2013; 447(1–2):231–40. <https://doi.org/10.1016/j.ijpharm.2013.02.048> PMID: 23467076
56. Park C-W, Son D-D, Kim J-Y, Oh T-O, Ha J-M, Rhee Y-S, et al. Investigation of formulation factors affecting in vitro and in vivo characteristics of a galantamine transdermal system. *International journal of pharmaceutics*. 2012; 436(1–2):32–40. <https://doi.org/10.1016/j.ijpharm.2012.06.057> PMID: 22771734
57. Zhao H, Park D-W, Kim S-K, Lee C-H, Kim D-D. The effects of pressure-sensitive adhesives and solubilizers on the skin permeation of testosterone from a matrix-type transdermal delivery system. *Drug development and industrial pharmacy*. 2002; 28(9):1125–31. <https://doi.org/10.1081/ddc-120014579> PMID: 12455471
58. Chaisson D. Dissolution Performance Testing Of Transdermal Systems. *Dissolution technologies*. 1995; 2(1):7–11.
59. Venkatraman S, Gale R. Skin adhesives and skin adhesion: 1. Transdermal drug delivery systems. *Biomaterials*. 1998; 19(13):1119–36. [https://doi.org/10.1016/s0142-9612\(98\)00020-9](https://doi.org/10.1016/s0142-9612(98)00020-9) PMID: 9720896
60. Mishra D, Ghosh G, Kumar PS, Panda PK. An experimental study of analgesic activity of selective COX-2 inhibitor with conventional NSAIDs. *Asian Journal of Pharmaceutical and clinical research*. 2011; 4(1):78–81.
61. Bentley G, Newton S, Starr J. Studies on the antinociceptive action of α -agonist drugs and their interactions with opioid mechanisms. *British journal of pharmacology*. 1983; 79(1):125–34. <https://doi.org/10.1111/j.1476-5381.1983.tb10504.x> PMID: 6135474
62. Morris CJ. Carrageenan-induced paw edema in the rat and mouse. *Inflammation protocols*: Springer; 2003. p. 115–21.
63. Smith WL, Marnett LJ. Prostaglandin endoperoxide synthase: structure and catalysis. *Biochimica et Biophysica Acta (BBA)-Lipids and Lipid Metabolism*. 1991; 1083(1):1–17.
64. Radhofer-Welte S, Rabasseda X. Lornoxicam, a new potent NSAID with an improved tolerability profile. *Drugs Today (Barc)*. 2000; 36(1):55–76.
65. Kusum Devi V, Saisivam S, Maria G, Deepti P. Design and evaluation of matrix diffusion controlled transdermal patches of verapamil hydrochloride. *Drug development and industrial pharmacy*. 2003; 29(5):495–503. <https://doi.org/10.1081/ddc-120018638> PMID: 12779279
66. Benecke AG, Kinne DJ, Wnuk AJ. Storage-stable transdermal patch. Google Patents; 1991.